

Results from a Hidden Photon Dark Matter Search Using a Multi-Cathode Counter

A. Kopylov,¹ I. Orekhov, V. Petukhov

Institute for Nuclear Research RAS,
prospect 60-letiya Otyabrya 7a, Moscow 117312, Russia

E-mail: beril@inr.ru

Abstract. The results of measurements are presented as rates of single electrons emitted from a cathode of a proportional counter filled with an argon–methane mixture. The results are interpreted as a possible photoelectric effect associated to hidden photons (HP). The upper limits have been set for hidden photons of cold dark matter (CDM). Also, future options for searches of HP of CDM using a multi-cathode counter technique are discussed.

¹Corresponding author.

Contents

1	Introduction	1
2	Measurement strategy	1
3	Apparatus	2
4	Data analysis	4
5	Summary	5

1 Introduction

To further the experimental efforts in the search of dark matter, physicists are looking now for new approaches. One such approach is using a dish antenna to observe hidden photons (HP) of cold dark matter (CDM) [1]. This technique has been realized [2], and an upper limit was set for HP mass, $m_{\gamma'} = 3.1 \pm 1.2$ eV. This range of masses was limited by the coefficient of reflection of light from a mirror and by the spectral sensitivity of a photomultiplier tube. At higher frequencies, the light is absorbed by the reflecting surface, which results in a loss of sensitivity of this technique. However, the absorption of higher-frequency light causes the emission of electrons from the surface if the energy of the photons is higher than the work function of the metal of the reflector. Hence, by counting single electrons emitted from the metal one can extend the sensitivity of this technique into vacuum ultraviolet range and higher. We developed a special detector for this study—a multi-cathode counter [3]. The first results of measurements using a counter with a copper cathode have been presented [4]. A new counter with an improved design using an aluminum cathode and focusing rings was used in measurements with an increased sensitivity [5]. Here we summarize the results of all of our measurements and outline our plans for further research.

2 Measurement strategy

If dark matter is totally composed of HPs, then the power collected by an antenna (here, by a cathode of the counter)

$$P = 2\alpha^2\chi^2\rho_{CDM}A_{cath} \quad (2.1)$$

where $\alpha = \cos(\theta)$ and θ is the angle between the direction of HP vector and the surface of the cathode, $\alpha^2 = 2/3$ if the HP vector is distributed randomly, $\rho_{CDM} \approx 0.3\text{GeV}/\text{cm}^3$ is the energy density of CDM, which is assumed to be equal to the energy density of the HPs, A_{cath} is the area of the cathode of the counter and χ is a dimensionless parameter quantifying the kinetic mixing [1]. If this power is converted into single electrons emitted from the cathode of the counter, then

$$P = m_{\gamma'} \cdot R_{MCC}/\eta \quad (2.2)$$

where $m_{\gamma'}$ is the mass (energy) of an HP, η is the quantum efficiency for a photon with energy $m_{\gamma'}$ to yield a single electron from the surface of the metal, and R_{MCC} is the rate of single electrons emitted from the cathode which is presumed here as being from HP. Thus, by combining (2.1) and (2.2) we obtain:

$$\chi_{\text{sens}} = 2.9 \cdot 10^{-12} \left(\frac{R_{MCC}}{\eta \cdot 1Hz} \right)^{\frac{1}{2}} \left(\frac{m_{\gamma'}}{1eV} \right)^{\frac{1}{2}} \left(\frac{0.3 \text{ GeV/cm}^3}{\rho_{CDM}} \right)^{\frac{1}{2}} \left(\frac{1m^2}{A_{MCC}} \right)^{\frac{1}{2}} \left(\frac{\sqrt{2/3}}{\alpha} \right) \quad (2.3)$$

Here it was assumed that the quantum efficiency η by absorption of the energy of HP by the surface of a metal cathode would be equal to the quantum efficiency for the real photon of the same energy. The sensitivity depends critically upon the dark rate of the counter. Single electrons can be emitted by any defects on the surfaces of the wires, protrusions, and spots of heterogeneity on the surface of a cathode sheet. Considering the abovementioned conditions, χ from (2.3) is only an upper limit. To improve the limit, we need to decrease a dark rate of the counter. One of the ways would be to apply a surface treatment to diminish the effect from extraneous sources. Another possibility would be to lower the temperature of the detector to diminish the contribution from thermionic emission, which depends on the work function ϕ_W of the metal and the temperature T in Kelvin, as expressed in the Richardson equation:

$$R_{\text{therm}} = a \cdot T^2 \cdot e^{-\frac{\phi_W}{kT}} \quad (2.4)$$

where R_{therm} is the thermionic dark rate, a is a constant and k is the Boltzmann constant. Using an Ar/CH_4 mixture enables to lower the temperature to $-40^\circ C$ what can substantially reduce a thermionic dark rate.

3 Apparatus

A schematic of a multi-cathode counter is presented in figure 1. The counter filled by Ar/CH_4 mixture has three cathodes and one anode made of gold-plated Tungsten-Rhenium wire of $25 \mu m$. The low (negative) potential HV1 is applied to the cathode 1 which is made of a metal sheet and we measure the rate of counting of individual electrons emitted from the surface of this sheet. The second cathode is 5 mm from the outer cathode. It consists of a series of nichrome wires of diameter $50 \mu m$ with a pitch of 4.5 mm. This cathode serves as a barrier for the electrons emitted from outer cathode. The potential HV2 applied to cathode 2 in configuration 1 is higher than HV1, so that electrons emitted from a cathode 1 can drift to the central counter with a cathode 3 of smaller diameter made of nichrome wires $50 \mu m$ with a pitch of 6 mm. The smaller (40 mm) diameter of a cathode 3 is used to get high ($\approx 10^5$) gas amplification to register the signal from single-electrons. In configuration 2 the potential HV2 is lower than HV1, so that electrons emitted from the outer cathode are scattered back from a cathode 2 and do not reach a central counter. In this configuration we measure the dark rate which is due to electrons emitted from wires and also from ionizing particles crossing the counter by short tracks at both ends. Both configurations have similar geometries and similar electric fields so that one can expect that by finding the difference of count rates $R_1 - R_2$ measured in these two configurations the net effect from the outer cathode is measured.

To reduce the background from gamma-radiation from the surrounding walls the counter has been placed in a special cabinet made of steel slabs of total thickness 30 cm. The measurements have shown that the count rate of single electrons outside a shield was higher than the one inside of a shield by about 20%. The attenuation of the gamma radiation by the shield was greater than a factor of 100 for a gamma with the energy of the peak of the gamma-spectrum measured by NaI(Tl) crystal which was about 200 keV. From here one obtains that the contribution of the single electron count rate from gamma radiation inside a shield is on the level of less than 0.2% of the single electron count rate inside a shield. No events have been observed coincident with muons crossing a detector. The rate R_{MCC} is obtained here as a difference between $R_1 - R_2$, the count rates in the two configurations with different potentials at the second cathode [3], see figure 1. We assumed that in configuration 1, the count rate is determined by the rate of emission of single electrons from the cathode of the counter, wires, and particles with short tracks crossing the counter at the both ends (the end effect). In configuration 2, the rate is determined by the rate of emission from the wires and the end effect. The exact contribution of the end effect and of the wires to the total count rate in configuration 2 is an unknown entity in this technique. This uncertainty is a main source of our systematic error.

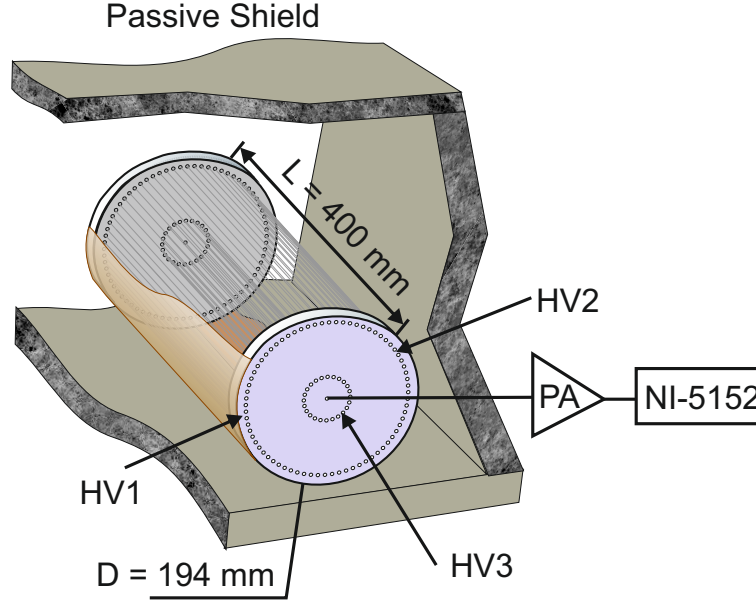


Figure 1. Schematic view of a multi-cathode counter in a shielded cabinet.

The number of electrons lost during diffusion from the outer cathode of the counter to central counter was estimated following mechanism of attachment proposed by Bloch and Bradbury and developed by Herzenberg (BBH model) [6, 7] for electrons of small energy. The number of free electrons in a gas which contains electronegative impurities (in our case this is an oxygen impurity) is decreasing exponentially:

$$N(t) = N(0) \cdot e^{-At} \quad (3.1)$$

here $N(t)$ – a number of electron at time t , $N(0)$ – the initial number of electrons, A – “the velocity of attachment”. The latter can be described by the expression

$$A = P(M) \cdot P(O_2) \cdot C_{O_2,M} \quad (3.2)$$

where $P(M)$, $P(O_2)$ – the pressure of working gas and the one of oxygen, $C_{O_2,M}$ – the coefficient of attachment, which does not depend upon the pressure of gas and of impurity in BBH model.

The field strength in our detector calculated by means of Maxwell16 is presented at figure 2.

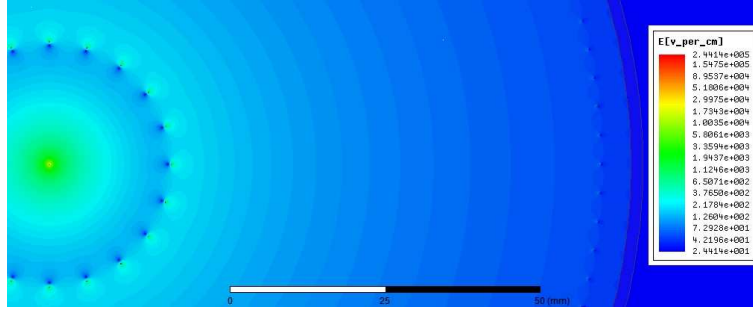


Figure 2. The calculated electric field strength across the counter.

From here, using the data on dependence of the drift velocity of electrons upon E/p in argon-methane mixture [6] and the one on coefficient of attachment $C_{O_2,M}$ from [7] one can determine the probability for electron to be attached while drifting on the way from outer cathode to a central counter. We obtained that for our gas mixture this probability was less than 1%, i.e. it can be neglected.

4 Data analysis

The pulse shapes were digitized in intervals of ± 50 mV with a frequency of 10 MHz and a sampling step of $400 \mu\text{V}$. Each measurement lasted for 12 h after which the data were processed offline. For the selection of “true” events a selection has been performed in space of three parameters: amplitude of the pulse, the duration of the leading edge of the pulse and a parameter β which describes prehistory of the event and is proportional to a first derivative of a baseline, approximated by a straight line during $50 \mu\text{sec}$ before leading edge of the pulse. The efficiency was estimated as the probability for the pulse to belong to ROI box of this 3-parameter space. It was found to be $(88 \pm 6)\%$. To reduce the influence of the noise on counting only intervals with a baseline deviation from zero not more than 5 mV were taken into account with a proper correction for a live time of counting which was found to be about 54%.

To evaluate the contribution to the total measured rate of the one of emission of electrons from wires we need to consider that in configuration 2 only the part of the surfaces of the wires facing the center of the counter produces the effect. Electrons emitted from the opposite parts are retarded by the potential of the second cathode and cannot drift toward the central counter. They are locked in the region between the first and second cathodes (figure 3). This will result in the reduced background measured in configuration 2. Instead, of $R_1 - R_2$, which

is true if the entire rate is due to the end effect, we should use in the case if the entire rate is due to the wires:

$$R_{MCC} = R_1 - \frac{n_3 + n_2}{n_3 + n_2/2} R_2 \quad (4.1)$$

This will produce a result lower than $R_1 - R_2$. Here n_2 and n_3 are the number of wires in the second and third cathodes, respectively, see [5].

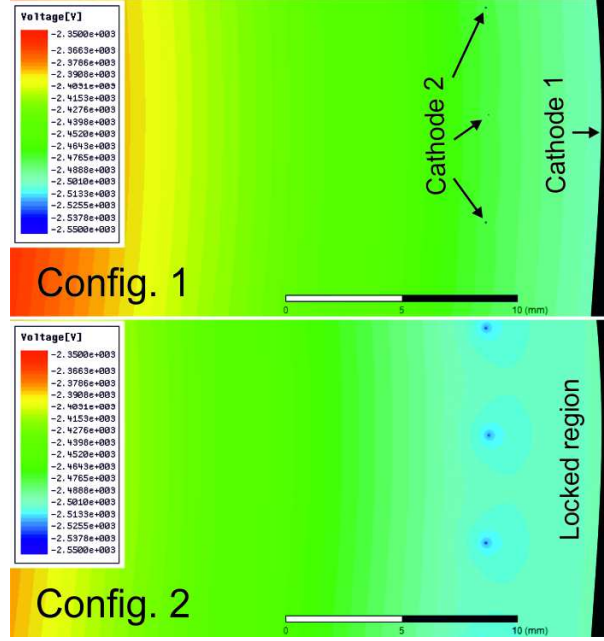


Figure 3. Calculated electric potentials across the counter for the two configurations.

5 Summary

A summary of the results of all the measurements is presented below. The limits at a 95% confidence levels are presented at figure 7. The limit Cu-1 was obtained from the results of [4] obtained by using a counter with a copper outer cathode at a room temperature. The limit Cu-2 was set based on measurements made at different temperatures (figure 4).

After selection of “true” pulses we obtained for $r_{MCC} = R_{MCC}/A_{cath}$: $(0.98 \pm 0.22) \cdot 10^{-4} Hz/cm^2$, $(0.75 \pm 0.15) \cdot 10^{-4} Hz/cm^2$ and $(0.69 \pm 0.23) \cdot 10^{-4} Hz/cm^2$ for these temperatures correspondingly (figure 5). The fact that the count rate was not revealing a clear increase with temperature can be taken as evidence that there was negligible contribution of thermal emission. As an average value for all these temperatures it was obtained: $r_{MCC} = (0.81 \pm 0.08) \cdot 10^{-4} Hz/cm^2$.

The limit Al-1 was obtained from the results of measurements presented in figure 6. We assumed that the main contribution to the rate is due to the end effect.

The average value found for all measurements presented at figure 6: $r_{MCC} = (0.8 \pm 0.25) \cdot 10^{-5} Hz/cm^2$. This is the lowest result obtained by this time. If we assume that electrons emitted from wires of the cathodes also contribute to the count rate, i.e. if to take

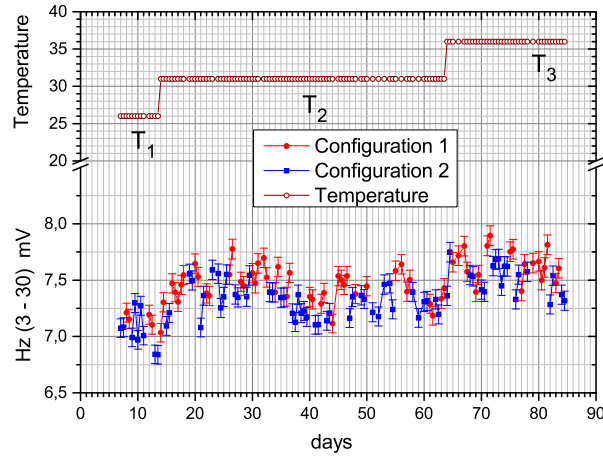


Figure 4. Results of measurements obtained using a counter with a copper cathode at different temperatures.

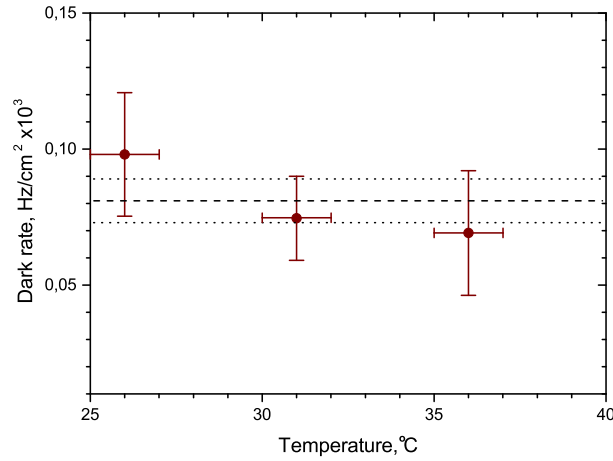


Figure 5. The distribution of events in sets 26°C, 31°C, 36°C. Dashed line – the average value obtained for all measurements, by point line are depicted levels $\pm 1\sigma$ from average value.

into account our systematic error, the curves for Cu-1, Cu-2, and Al-1 in figure 7 would be set lower. An advanced surface treatment could further improve the sensitivity of the measurements.

Good progress has been made by using the counter with an aluminum cathode. Further improvements could be made by using Ni or Pt as a metal with a higher work function for cathode of the counter and by applying a more advanced surface treatment. One can see from figure 7 that our limits are still higher than the limits given by a solar lifetime. Hence we should make a significant improvement to go beyond these limits. However one should also take into account the possible uncertainties in the models relevant for the two processes:

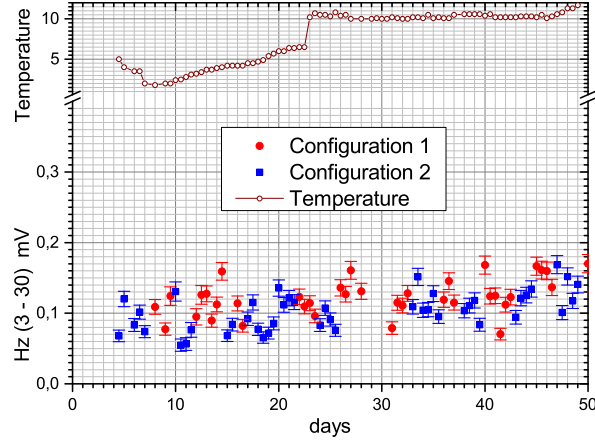


Figure 6. Results of measurements obtained using a counter with an aluminum cathode.

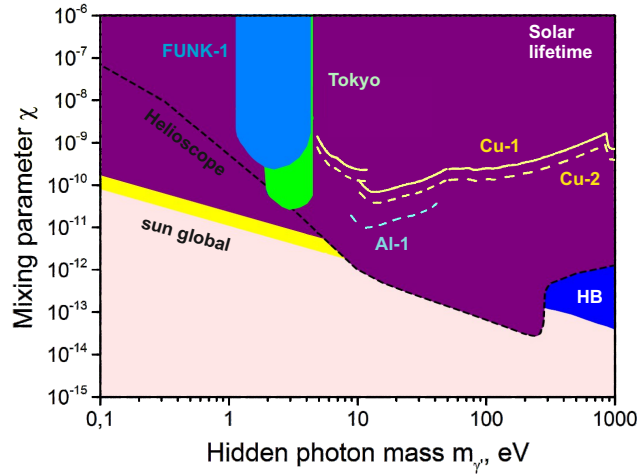


Figure 7. Limits at a 95% CL obtained from a series of measurements Cu-1, Cu-2, and Al-1. Here limits Tokyo are from [2] and FUNK-1 from [10].

inside the Sun with the emission of photon and on the surface of a metal with the emission of electron. The important thing of this work is that the limits have been obtained by us in direct measurements.

Acknowledgments

The work was funded by the Federal Agency for Scientific Organizations, Russia.

References

- [1] D Horns, J Jaeckel, A Lindner et al., *Searching for WISPy cold dark matter with a dish antenna*, *JCAP* **04** (2013) 016.
- [2] J Suzuki, T Horie, Y Inoue, and M Minowa, *Experimental search for hidden photon CDM in the eV mass range with a dish antenna*, *JCAP* **09** (2015) 42.
- [3] A V Kopylov, I V Orekhov, V V Petukhov, *A method to register hidden photons with the aid of a multi-cathode counter*, *Tech. Phys. Lett.* **42** (2016) 879
- [4] A V Kopylov, I V Orekhov, V V Petukhov, *On a Search for Hidden Photon CDM by a Multicathode Counter*, *Advances In High Energy Phys.* **2016** (2016) 2058372
- [5] A Kopylov, I Orekhov, V Petukhov, *A multi-cathode counter in a single-electron counting mode*, *NIM A* **910** (2018) 164.
- [6] Bloch F. and Bradbury N., *On the mechanism of unimolecular electron capture*, *Phys. Rev.* **48** (1935) 689.
- [7] A. Herzenberg, *Attachment of Slow Electrons to Oxygen Molecules*, *J. Chem. Phys.* **51** (1969) 4942.
- [8] Alan A. Sebastian and J.M. Wadehra, *Time-dependent behaviour of electron transport in methane-argon mixtures* *J. Phys. D Appl. Phys.* **38** (2005) 1577
- [9] M. Huk, P. Igo-Kemenes and A. Wagner, *Electron attachment to oxygen, water, and methanol, in various drift chamber gas mixtures*, *NIM A* **267** (1988) 107.
- [10] R Engel, Veberič, C Schäfer et al., *Search for hidden-photon Dark Matter with FUNK*, *arXiv:1711.02961v1 [hep-ex]*